Original Article | Breast Imaging

eISSN 2005-8330
https://doi.org/10.3348/kjr.2019.0881
Korean J Radiol 2020;21(11):1210-1219

Korean Journal of Radiology
KJR

Utility and Diagnostic Performance of Automated Breast Ultrasound System in Evaluating Pure Non-Mass Enhancement on Breast Magnetic Resonance Imaging

Bo Ra Kwon, MD[1, 2], Jung Min Chang, MD[1], Soo-Yeon Kim, MD[1], Su Hyun Lee, MD[1], Sung Ui Shin, MD[1, 2], Ann Yi, MD[2], Nariya Cho, MD[1], Woo Kyung Moon, MD[1]

[1]Department of Radiology, Seoul National University Hospital, Seoul National University College of Medicine, Seoul, Korea; [2]Department of Radiology, Seoul National University Hospital Healthcare System Gangnam Center, Seoul, Korea

Objective: To compare the utility and diagnostic performance of automated breast ultrasound system (ABUS) with that of hand-held ultrasound (HHUS) in evaluating pure non-mass enhancement (NME) lesions on breast magnetic resonance imaging (MRI).
Materials and Methods: One hundred twenty-six consecutive MRI-visible pure NME lesions of 122 patients with breast cancer were assessed from April 2016 to March 2017. Two radiologists reviewed the preoperative breast MRI, ABUS, and HHUS images along with mammography (MG) findings. The NME correlation rate and diagnostic performance of ABUS were compared with that of HHUS, and the imaging features associated with ABUS visibility were analyzed.
Results: Among 126 pure NME lesions, 100 (79.4%) were malignant and 26 (20.6%) were benign. The overall correlation rate was 87.3% (110/126) in ABUS and 92.9% (117/126) in HHUS. The sensitivity and specificity were 87% and 50% for ABUS and 92% and 42.3% for HHUS, respectively, with no significant differences (p = 0.180 and 0.727, respectively). Malignant NME was more frequently visualized than benign NME lesions on ABUS (93% vs. 65.4%, p = 0.001). Significant factors associated with the visibility of ABUS were the size of NME lesions on MRI (p < 0.001), their distribution pattern (p < 0.001), and microcalcifications on MG (p = 0.027).
Conclusion: ABUS evaluation of pure NME lesions on MRI in patients with breast cancer is a useful technique with high visibility, especially in malignant lesions. The diagnostic performance of ABUS was comparable with that of conventional HHUS in evaluating NME lesions.
Keywords: *Automated breast ultrasound system; Magnetic resonance imaging; Non-mass enhancement; Visibility; Diagnostic performance; Breast cancer*

INTRODUCTION

Non-mass enhancement (NME) is defined as an area of enhancement without an associated space-occupying mass or focus in the Breast Imaging Reporting and Data System (BI-RADS) lexicon of the American College of Radiology. It is generally different from the normal surrounding background parenchymal enhancement (1). NME is a common finding during screening and diagnostic magnetic resonance imaging (MRI) examinations. These lesions are characterized by their distribution, internal enhancement pattern, and symmetry; however, the differential diagnosis of NME on MRI is not always simple because of the substantial overlap among benign, high-risk, and malignant

Received: December 17, 2018 **Revised:** March 11, 2020 **Accepted:** March 29, 2020
This research was supported by a grant of the Korea Health Technology R&D Project through the Korea Health Industry Development Institute (KHIDI), funded by the Ministry of Health & Welfare, Republic of Korea (grant number: HI15C1532).
Corresponding author: Jung Min Chang, MD, Department of Radiology, Seoul National University Hospital, 101 Daehak-ro, Jongno-gu, Seoul 03080, Korea.
• E-mail: imchangjm@gmail.com

Korean Journal of Radiology
KJR

lesions. Segmental or clumped, and linear enhancements are frequent manifestations of ductal carcinoma *in situ* (DCIS); however, these can also be found in benign diseases, such as fibrocystic changes, mammary duct ectasia, and sclerosing adenosis (2-5).

Lesions detected using breast MRI and considered suspicious should be biopsied for histopathological confirmation. Although MRI-guided biopsy is a safe and accurate diagnostic tool, there are certain limitations to its broad application owing to its cost, availability, and requirement for contrast medium administration (6-8). Breast ultrasound (US) is commonly used for targeted evaluation of a lesion or lesions initially identified on MRI. It can help in decision making in clinical practice by characterizing or localizing the MRI-detected lesion and obtaining pathological results with US-guided biopsy instead of MRI-guided biopsy (9). However, conventional hand-held US (HHUS) has disadvantages including operator dependency and poor reproducibility (10).

The automated breast US system (ABUS) is a recently introduced US technique aimed to overcome the limitations of HHUS (11). This system permits the entire examination to be stored and read, whenever necessary (12). Considering that ABUS provides three-dimensional whole breast data, correlation with NME on MRI can be more straightforward. Correlation rates for NME on HHUS are reported to vary from 0% to 54% (13-16), suggesting it to be less likely for NME to have a correlate than a mass or focus (9, 17-19). However, only limited studies have specifically investigated the utility of ABUS to evaluate NME lesions on MRI. Therefore, the present study compared the utility and diagnostic performance of ABUS with HHUS in evaluating pure NME lesions on MRI.

MATERIALS AND METHODS

Study Population

The institutional review board of the authors' institution approved the review of images and medical records. Furthermore, it waived the requirement for obtaining informed consents from patients because the study was performed retrospectively on routinely acquired preoperative images using breast MRI, ABUS, and HHUS.

Since 2016, ABUS has been performed in Seoul National University Hospital for preoperative imaging work-up to evaluate the tumor extent or multiplicity in patients diagnosed with breast cancer. In addition, HHUS is performed simultaneously in all patients for marking or localizing the lesions. Between April 2016 and March 2017, preoperative breast MRI was performed on 1491 consecutive breast cancer patients. Only patients with at least one BI-RADS category 0, 4, or 5 NME lesions (n = 388) on MRI were included. Among them, females who received neoadjuvant chemotherapy (n = 72) or underwent excisional biopsy (n = 25) or did not undergo ABUS (n = 34) were excluded. In addition, 131 cases with findings of mass lesions associated with NME were excluded to evaluate pure NME. Finally, 126 pure NME breast lesions in 122 patients (mean age 52 years [range: 30–76 years]) were included in the present study.

Image Acquisition

During the study period, preoperative dynamic breast MRI examinations were performed with the patient in the prone position, using a 3T scanner with one of the two different systems (Ingenia 3T CX; Philips Healthcare; Magnetom Skyra; Siemens Healthineers) equipped with a dedicated breast coil. The imaging sequences included a three-plane localizing sequence; fat-suppressed T2-weighted images; diffusion-weighted images; and dynamic T1-weighted, fat-suppressed images including pre-contrast acquisition and five post-contrast dynamic series after intravenous administration of a bolus (0.1 mmol/L per kg of body weight) of gadobutrol (Gadovist; Bayer AG). Post-processing, including subtraction images, sagittal and coronal reconstructed images, and maximum intensity projections, was routinely used.

ABUS images were acquired by two trained technologists using a standardized scanning technique on an ABUS unit (Invenia ABUS; GE Healthcare). The patients were positioned supine with the arm of the side under examination placed over their head. Each breast was scanned separately in three views: anterior–posterior, lateral, and medial, while the transducer was applied to the breast with tender compression. In cases involving larger breasts, superior and/or inferior views were added to adequately cover sufficient breast tissue. All views used the nipple as the reference point. A layer of lotion was used to ensure adequate contact with the skin of the entire breast. The time required to obtain ABUS data ranged from 6 to 9 min per breast.

Image Review and Data Analysis

Clinical and pathological findings from biopsy or surgery were collected from electronic medical records. Preoperative

 https://doi.org/10.3348/kjr.2019.0881

MRI examinations were reviewed by a radiologist, who specialized in breast imaging, and indeterminate or suspicious (BI-RADS category 0 or over 4A) pure NME lesions were verified using medical records. The imaging characteristics of pure NME lesions on MRI, including distribution (focal, linear, segmental, regional, multiple regions, and diffuse), patterns of internal enhancement (homogeneous, heterogeneous, clumped, and clustered ring), and BI-RADS assessment category, were recorded (1). Subsequently, ABUS data were reviewed by two radiologists independently after reviewing MR NME and without final pathology or follow-up imaging data. The presence or absence of a corresponding lesion was evaluated. ABUS imaging findings were described and the BI-RADS final category was determined in the presence of a corresponding lesion (20). The ABUS imaging findings, including the lesion shape (oval/round or irregular), margin (circumscribed, indistinct, lobulated, spiculated), echogenicity (hyperechoic, isoechoic, hypoechoic, heterogeneous), and size (maximum diameter) of the correlated lesion, were evaluated. For HHUS evaluation, we retrospectively collected HHUS data to determine BI-RADS final categories for comparison with ABUS. Furthermore, the mammographic information was provided, and associated imaging characteristics, such as architectural distortion and microcalcifications, were evaluated (21). Difference of opinion between readers was addressed by reassessing the lesion in consensus to record the best concordant results. With regard to clinical management, HHUS was performed in all cases to identify the correlating lesion, and US- or MRI-guided biopsy was performed for suspicious NME, irrespective of its visibility on ABUS. Outcomes were assessed based on biopsy, surgical pathological results, or 1-year follow-up data. Follow-up examinations performed between 9 and 15 months after the last imaging date were considered as 1-year follow-up. The correlation rate of pure NME lesions on ABUS was calculated, and the difference in benign and malignant NME lesions was evaluated separately on the basis of pathology or follow-up data. In addition, the associated imaging features related to ABUS visibility were analyzed. Categorical variables associated with malignancy were compared using the chi-squared tests. To compare the diagnostic performance between ABUS and HHUS, the BI-RADS category 4A was used as the cut-off point to distinguish malignant (categories 4A or higher) and benign (categories 1, 2, and 3) lesions for correlated lesions. The sensitivity, specificity, and accuracy of ABUS and HHUS were calculated. McNemar's test was used to analyze the difference in sensitivity, specificity, and accuracy of two modalities. A p-value < 0.05 was considered as statistically significant. Statistical analyses were performed using the SPSS version 21.0 (IBM Corp.).

RESULTS

Pathology and Imaging Characteristics of NME

Among 126 pure NME lesions in 122 patients, 100 lesions (79.4%) were malignant and 26 lesions (20.6%) were benign. The malignancies were invasive ductal carcinoma in 48 lesions, DCIS in 46 lesions, and invasive lobular carcinoma in 6 lesions; all lesions underwent breast cancer surgery including mastectomy (n = 74) and breast conserving surgery (n = 26). The mean size of invasive tumor was 8.1 ± 13.0 mm, and the mean size of invasive tumor combined with DCIS was 41.6 ± 22.1 mm. Among the 100 malignant NME lesions, 95 were known breast cancer and 5 were incidental findings of MRI in ipsilateral (n = 3) or contralateral (n = 2) breasts. Pathological confirmations were achieved after US-guided biopsy in 79 lesions, stereotactic biopsy in 3, MR-guided biopsy in 1, and excisional biopsy with US-guided localization in 2 lesions. The remaining 15 lesions were confirmed via breast cancer surgery without biopsy. Among the 26 benign NME lesions, 10 lesions were confirmed by US-guided biopsy, 3 lesions by excisional biopsy with US-guided localization, and 6 lesions by breast cancer surgery, and the remaining 7 lesions were confirmed as benign with 1-year follow-up using US and/or MRI examinations.

Regarding MRI findings, the distribution of NME lesions was focal in 33 lesions, linear in 13 lesions, segmental in 67 lesions, and diffuse in 13 lesions. Internal enhancement patterns were homogeneous in 3 lesions, heterogeneous in 50 lesions, clumped in 46 lesions, and clustered ring in 27 lesions. Final assessments on MRI included 5 category 0 lesions, 25 category 4A lesions, 24 category 4B lesions, 18 category 4C lesions, and 54 category 5 lesions. Mammographic breast density revealed 16 fatty breasts (breast compositions a and b) and 110 dense breasts (c and d) (21). MG findings were negative in 48 lesions, mass in 8 lesions, asymmetry in 11 lesions, architectural distortion in 4 lesions, and combined microcalcifications in 55 lesions. A comparison of MRI features between benign and malignant NME lesions is presented in Table 1. The size of pure NME lesions on MRI ranged from 0.6 to 9.3 cm, with a mean of

https://doi.org/10.3348/kjr.2019.0881

Korean Journal of Radiology
KJR

2.4 cm for benign lesions and 4.7 cm for malignant lesions. When the NME lesion size on MRI was divided into three categories: < 2 cm, ≥ 2 cm and < 5 cm, and ≥ 5 cm, there was a tendency toward increased malignancy as the lesion size increased (p < 0.001). Among the 126 pure NME lesions on MRI, distribution (linear [10/13, 76.9%], segmental [62/67, 92.5%], and diffuse [12/13, 92.3%]) and enhancement patterns (clumped [42/46, 91.3%] and clustered ring [26/27, 96.3%]) were significant predictors of malignancy (p < 0.001, respectively). Other significant radiological features predictive of malignancy were asymmetry (10/11 [90.9%]) and combined microcalcifications (53/55 [96.4%]) on MG (p < 0.001). However, there was no association between breast density, background parenchymal enhancement, and malignant NME (Table 1).

Table 1. Comparison of MRI and Mammographic Features between Benign and Malignant NME Lesions

Imaging Findings	Benign (n = 26)	Malignant (n = 100)	*P*
MRI findings			
FGT			0.849
a	0 (0)	3 (3)	
b	6 (23.1)	22 (22)	
c	13 (50.0)	49 (49)	
d	7 (26.9)	26 (26)	
BPE			0.606
Minimal	10 (38.5)	37 (37)	
Mild	6 (23.1)	35 (35)	
Moderate	5 (19.2)	16 (16)	
Marked	5 (19.2)	12 (12)	
Size (cm)			< 0.001
< 2	12 (46.2)	12 (12)	
2–5	12 (46.2)	42 (42)	
> 5	2 (7.6)	46 (46)	
Distribution			< 0.001
Focal	17 (65.4)	16 (16)	
Linear	3 (11.5)	10 (10)	
Segmental	5 (19.2)	62 (62)	
Diffuse	1 (3.9)	12 (12)	
Patterns			< 0.001
Homogeneous	1 (3.9)	2 (2)	
Heterogeneous	20 (76.8)	30 (30)	
Clumped	4 (15.4)	42 (42)	
Clustered ring	1 (3.9)	26 (26)	
MG findings			< 0.001
Negative	23 (88.4)	25 (25)	
Mass	0 (0)	8 (8)	
Asymmetry	1 (3.9)	10 (10)	
Distortion	0 (0)	4 (4)	
Microcalcifications	2 (7.6)	53 (53)	

Data are number of patients, with percentage in parentheses. a = almost entirely fat, b = scattered fibroglandular tissue, BPE = background parenchymal enhancement, c = heterogeneous fibroglandular tissue, d = extreme fibroglandular tissue, FGT = fibroglandular tissue, MG = mammographic, NME = non-mass enhancement

Lesion Visibility and Diagnostic Performance of NME on ABUS and HHUS

Among 126 pure NME lesions, 117 NME lesions (92.9%) were identified on HHUS, and 110 lesions (87.3%) were visualized on ABUS. The correlation rate of NME lesions on HHUS was higher than that on ABUS; however, it was not statistically significant (p = 0.065). There were 23 discrepant assessments regarding ABUS visibility between the two readers; these cases were reassessed by consensus. ABUS correlation was observed in 93 (93%) of 100 malignant lesions and 17 (65.4%) of 26 benign lesions (p = 0.001). Sixteen NME lesions (12.7%) could not be identified on ABUS; of these, seven were malignant and nine were benign lesions. Among the seven malignant lesions, that could not be identified on ABUS, two were confirmed via US-guided biopsy after diagnostic HHUS and the other five via breast cancer surgery. Out of nine benign lesions, three were confirmed by US-guided biopsy, three by surgical excision, and the remaining three were confirmed as benign by follow-up breast US and MRI without interval change of at least 1 year. Nine NME lesions could not be identified on HHUS, five were malignant, and four were benign lesions. All malignancies were confirmed via breast cancer surgery and remaining four NME lesions were confirmed as benign by follow-up breast MRI without change for at least 1 year. Results of the BI-RADS category in these modalities are shown in Table 2. The overall diagnostic performances of ABUS and HHUS were compared in Table 3. The sensitivity, specificity, and accuracy of ABUS were 87%, 50%, and 79.4%, respectively, and those of HHUS were 92%, 42.3%, and 81.8%, respectively; the differences were not statistically significant (p = 0.180, 0.727, and 0.143, respectively).

Imaging Features Associated with ABUS Visibility

ABUS correlation was observed more frequently in NME lesions with size ≥ 2 cm than in those with size < 2 cm, showing better correlation with a progressive increase in lesion size (p < 0.001). The distribution of NME was associated with ABUS visibility; the segmental distribution

https://doi.org/10.3348/kjr.2019.0881

demonstrated a higher frequency of visualization (p < 0.001). Moreover, combined microcalcification on MG was associated with ABUS visibility (p = 0.027) (Table 4, Figs. 1, 2). However, internal enhancement patterns of NME were not associated with ABUS visibility (p = 0.103).

Table 2. Correlation and Results of BI-RADS Category by ABUS and HHUS

BI-RADS Category	ABUS	HHUS
Correlated	110 (87.3)	117 (92.8)
Category 3	10 (7.9)	10 (7.9)
Category 4A	47 (37.3)	47 (37.3)
Category 4B	27 (21.4)	33 (26.2)
Category 4C	20 (15.9)	18 (14.3)
Category 5	6 (4.8)	9 (7.1)
Not correlated	16 (12.7)	9 (7.1)
Total	126 (100)	126 (100)

Data are number of lesions, with percentage in parentheses. ABUS = automated breast ultrasound system, BI-RADS = Breast Imaging Reporting and Data System, HHUS = hand-held ultrasound

Among the 110 NMEs that were identified on ABUS, the final BI-RADS category of ABUS was significantly correlated with the pathology (p = 0.046). However, lesion size, lesion shape, margin, and echogenicity on ABUS did not show any significant difference between the benign and malignant lesions (p > 0.05) (Table 5).

DISCUSSION

The results of our study suggest that ABUS evaluation of pure NME on MRI in patients with breast cancer has

Table 3. Diagnostic Performance of ABUS and HHUS in Evaluating Pure NME on Breast MRI

	ABUS	HHUS	*P*
Sensitivity (%)	87.0 (78.8–92.9)	92.0 (84.8–96.5)	0.180
Specificity (%)	50.0 (29.9–707.1)	42.3 (23.4–63.1)	0.727
Accuracy (%)	79.4 (71.3–86.1)	81.8 (73.9–88.1)	0.143

Standard deviation are given in parentheses.

Table 4. Visibility of 126 Pure NME on MRI by Pathology and Imaging Findings

Variables	Visible on ABUS (n = 110)	Non-Visible on ABUS (n = 16)	*P*
Pathology			0.001
Benign lesions	17 (15.5)	9 (56.2)	
Malignancy	93 (84.5)	7 (43.8)	
IDC	47 (42.7)	1 (6.3)	
DCIS	40 (36.4)	6 (37.5)	
Others	6 (5.4)	0 (0)	
MRI findings			
NME size (cm)			< 0.001
< 2	14 (12.7)	12 (75.0)	
2–5	50 (45.5)	2 (12.5)	
> 5	46 (41.8)	2 (12.5)	
Distribution			< 0.001
Focal	23 (20.9)	10 (62.5)	
Linear	9 (8.2)	4 (25.0)	
Segmental	65 (59.1)	2 (12.5)	
Diffuse	13 (11.8)	0 (0)	
Pattern			0.103
Homogeneous	2 (1.8)	1 (6.25)	
Heterogeneous	40 (36.4)	10 (62.5)	
Clumped	42 (38.2)	4 (25.0)	
Clustered ring	26 (23.6)	1 (6.25)	
MG density			0.330
Non-dense	13 (11.8)	3 (18.7)	
Dense	97 (88.2)	13 (81.3)	
MG finding			0.027
With microcalcifications	52 (47.3)	3 (18.8)	
Without microcalcifications	58 (52.7)	13 (81.2)	

Data are number of patients, with percentage in parentheses. DCIS = ductal carcinoma *in situ*, IDC = invasive ductal carcinoma

https://doi.org/10.3348/kjr.2019.0881

Korean Journal of Radiology
KJR

comparable visibility and diagnostic performance with those obtained on HHUS. Furthermore, the visibility on ABUS was especially higher in malignant lesions. Despite segmental, clumped, or linear NME are more frequently noted in DCIS than in benign lesions (2, 4, 22), finding NME lesions on MRI is challenging owing to a high proportion of false-positive findings, ranging from 40% to 50% (2, 23). Once an NME lesion is detected on MRI, breast US can play a key role in work-up and management. However, in contrast to the reported rate of US correlation for masses (49–92%), most previous studies have reported that the yield for NME–US correlation is low and variable (0–54%) in second-look settings (14-16, 24, 25). Similarly, Hsu et al. (24) reported that second-look HHUS identified 43% of NME lesions, with

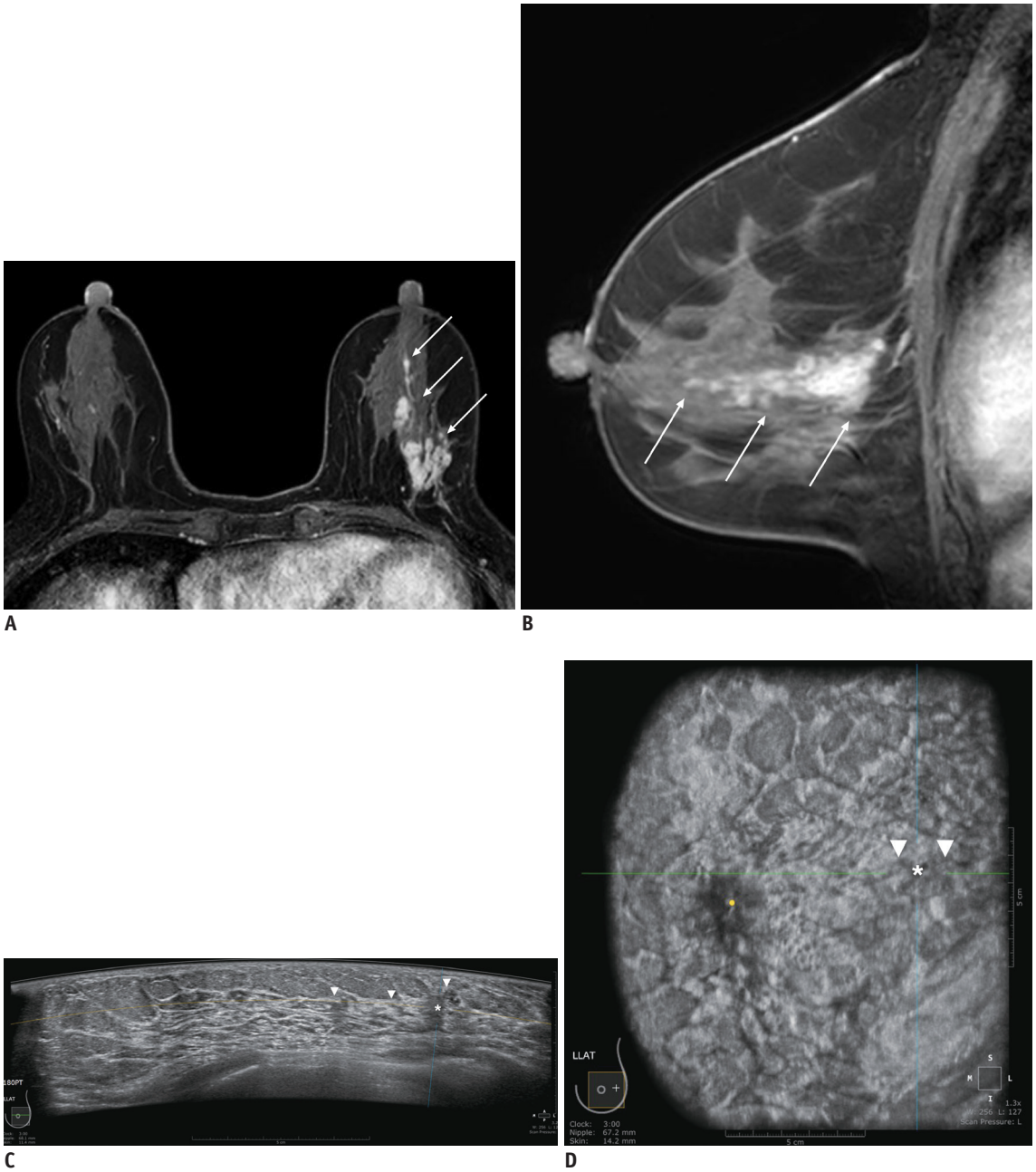

Fig. 1. 59-year-old female with left breast cancer who underwent MRI and ABUS for preoperative staging. Axial **(A)** and sagittal **(B)** dynamic contrast-enhanced MRI show segmental, heterogeneous non-mass enhancements (arrows) at left upper outer breast. ABUS images show ill-defined hypoechoic mass (asterisk) with ductal changes (arrowheads) on axial **(C)** and coronal **(D)** planes of left breast. Lesion measured 2.8 cm on ABUS and 5.8 cm on MRI. Mass was classified as BI-RADS category 4B. This patient subsequently underwent left modified radical mastectomy, and finally confirmed to have microinvasive carcinoma in background of DCIS. ABUS = automated breast ultrasound system, BI-RADS = Breast Imaging Reporting and Data System, DCIS = ductal carcinoma *in situ*

https://doi.org/10.3348/kjr.2019.0881

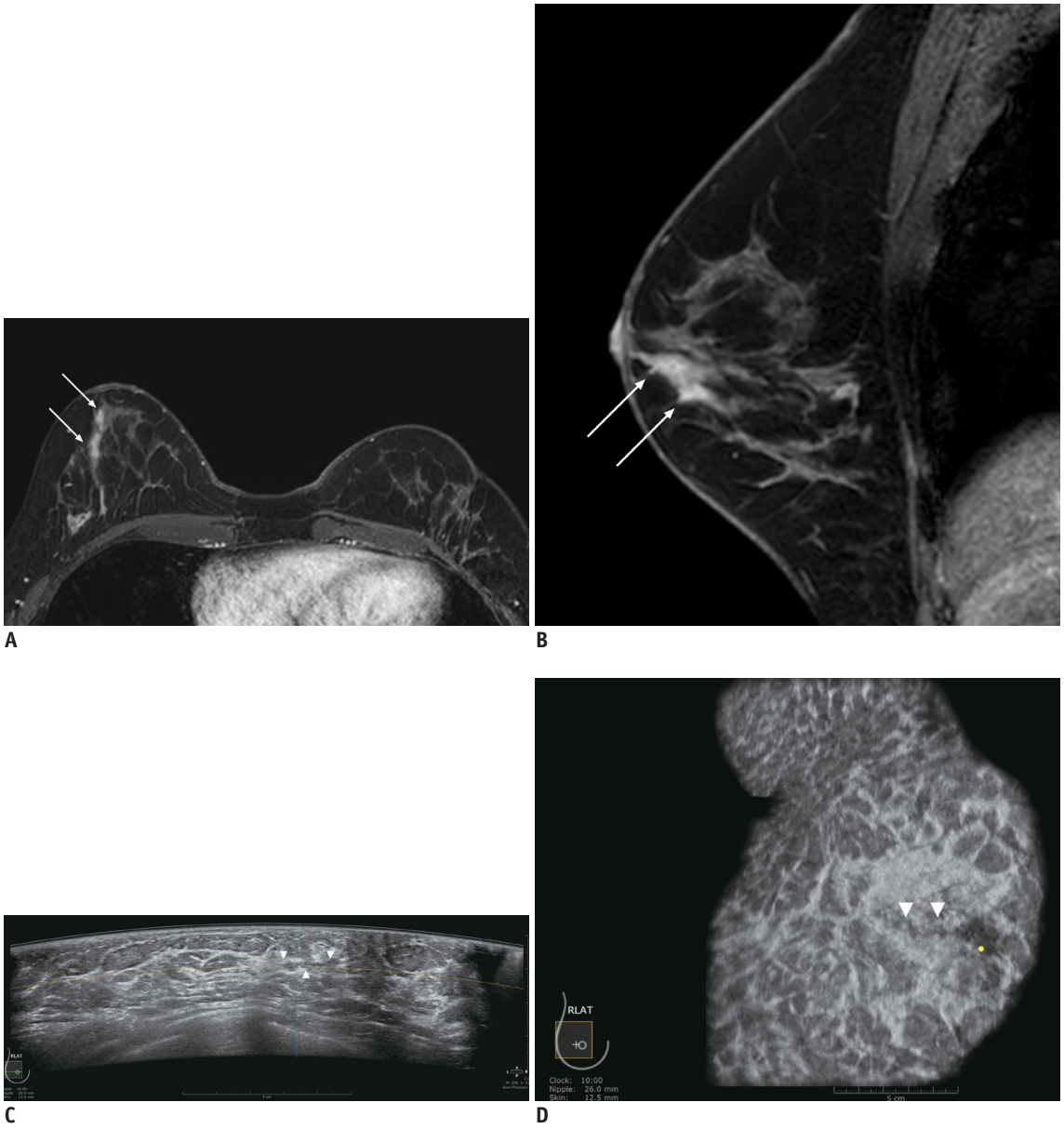

Fig. 2. 45-year-old female with right breast cancer who underwent MRI and ABUS for preoperative staging. Axial **(A)** and sagittal **(B)** dynamic contrast-enhanced MRI show linear, heterogeneous non-mass enhancements (arrows) at right outer subareolar region. ABUS images show ill-defined, indistinct lesion (arrowheads) on axial **(C)** and coronal **(D)** planes of right breast. Lesion measured 1.7 cm on ABUS and 2.8 cm on MRI. Mass was classified as BI-RADS category 4A. This patient subsequently underwent US-guided biopsy, and confirmed to usual ductal hyperplasia.

a correlation rate of 76% in malignant lesions compared with 18% in benign lesions.

Recent data regarding ABUS for evaluating MR-detected masses yielded a detection rate comparable with HHUS as a second-look procedure after MRI (69.3% and 71.5%, respectively), with perfect agreement (k = 0.94) in assessing significant lesions (26). Kim et al. (27) reported that the detection rate of the ABUS was higher than that of HHUS with regard to the second-look examination (94.7% vs. 86.8%); however, both techniques demonstrated specific limitations with regard to NME detection. The diagnostic performance of ABUS in evaluating NME has not been extensively investigated until date. Superior visibility with diagnostic performance could be expected as it provides three-dimensional whole-breast volume data with superior objectivity and reproducibility (28, 29). However, in our study, the lesion visibility and sensitivity of ABUS were lower than those of HHUS with no statistically significant difference. Although it was not a real second-look procedure, 87% of NME on MRI demonstrated a correlating

https://doi.org/10.3348/kjr.2019.0881

Korean Journal of Radiology
KJR

Table 5. ABUS Findings of Pure NME on MRI

ABUS Findings	Benign (n = 17)	Malignant (n = 93)	*P*
Size (cm)			0.291
< 2	8 (47.1)	32 (34.4)	
2–5	9 (52.9)	51 (54.8)	
> 5	0 (0)	10 (10.8)	
Lesion shape			0.457
Oval/Round	0 (0)	3 (3.2)	
Irregular	17 (100)	90 (96.8)	
Margin			0.877
Indistinct	16 (94.1)	88 (94.6)	
Lobulated	0 (0)	1 (1.1)	
Spiculated	1 (5.9)	4 (4.3)	
Echogenicity			0.203
Isoechoic	4 (23.5)	10 (10.8)	
Heterogeneous	5 (29.4)	20 (21.5)	
Hypoechoic	8 (47.1)	63 (67.7)	
BI-RADS category			0.046
Non-suspicious	4 (23.5)	6 (6.5)	
Suspicious	13 (76.5)	87 (93.5)	

Data are number of patients, with percentage in parentheses.

lesion on ABUS, which is a relatively higher rate than that reported in previous studies using HHUS (14-16, 24, 25) and ABUS (27). The reason for the higher correlation rate could be attributed to differences in the study population, considering the large number of malignant cases.

Furthermore, our study demonstrated that the visibility on ABUS was significantly associated with pathology, lesion size, NME distribution on MRI, and combined microcalcifications on MG, showing results similar to those of previous reports (5, 18, 22, 24, 30, 31). However, Newburg et al. (15) reported that no statistical difference was detected in the malignancy rate between NME with (18%) and without (12%) a correlate, which was different from the result obtained in our study. Indeed, NME with no US correlation does not exclude malignancy. In our study, 7 (IDC, n = 5; DCIS, n = 2) of 100 cancers could not be identified via ABUS. Among these, one case exhibited suspicious microcalcifications on MG, three showed suspicious findings on diagnostic HHUS, and the remaining three lesions were visible only on MRI. Furthermore, two lesions identified by diagnostic HHUS were confirmed by preoperative US-guided biopsy. The other five lesions were diagnosed by breast cancer operation without biopsy.

Our study had several limitations. First, it was a retrospective study with single-center design. However, ABUS examination, contrary to HHUS, is always interpreted after the examination, suggesting that our results may not demonstrate a significant difference from those of a prospective ABUS study. Second, the study population was limited to patients diagnosed with breast cancer; therefore, the rate of ABUS correlation could be different in screening patients. Third, we only included patients with indeterminate or suspicious NME on breast MRI. Benign or probable benign NME could show different correlation rates on ABUS. Fourth, follow-up MRI was not performed for all pure NME lesions, and follow-up studies, including MG or US, were used to confirm the stability of the lesions. Finally, the correlation between ABUS features and pathological findings, including the immunohistochemical subtypes of breast cancer, could not be evaluated owing to the small number of pure NME lesions.

In conclusion, the ABUS evaluation of pure NME lesions on MRI in patients with breast cancer is feasible, with a considerably high visibility rate, particularly in malignant lesions. ABUS is not inferior to conventional HHUS and could be used in evaluating NME lesions with advantage of three-dimensional evaluation. Further prospective studies are required to determine the role and diagnostic performance of ABUS as a second-look imaging modality to analyze NME lesions in comparison with HHUS.

Conflicts of Interest

The authors have no potential conflicts of interest to disclose.

ORCID iDs

Jung Min Chang
https://orcid.org/0000-0001-5726-9797
Bo Ra Kwon
https://orcid.org/0000-0002-7687-8800
Soo-Yeon Kim
https://orcid.org/0000-0001-8915-3924
Su Hyun Lee
https://orcid.org/0000-0002-0171-8060
Sung Ui Shin
https://orcid.org/0000-0001-6049-8419
Ann Yi
https://orcid.org/0000-0001-9103-0309
Nariya Cho
https://orcid.org/0000-0003-4290-2777
Woo Kyung Moon
https://orcid.org/0000-0001-8931-3772

 https://doi.org/10.3348/kjr.2019.0881

REFERENCES

1. Morris EA, Comstock CE, Lee CH, Lehman CD, Ikeda DM, Newstead GM, et al. ACR BI-RADS(R) magnetic resonance imaging. In: American College of Radiology, eds. *ACR BI-RADS(R) atlas, breast imaging reporting and data system*. Reston: American College of Radiology, 2013:12-21
2. Liberman L, Morris EA, Lee MJ, Kaplan JB, LaTrenta LR, Menell JH, et al. Breast lesions detected on MR imaging: features and positive predictive value. *AJR Am J Roentgenol* 2002;179:171-178
3. Tozaki M, Fukuda K. High-spatial-resolution MRI of non-masslike breast lesions: interpretation model based on BI-RADS MRI descriptors. *AJR Am J Roentgenol* 2006;187:330-337
4. Morakkabati-Spitz N, Leutner C, Schild H, Traeber F, Kuhl C. Diagnostic usefulness of segmental and linear enhancement in dynamic breast MRI. *Eur Radiol* 2005;15:2010-2017
5. Thomassin-Naggara I, Trop I, Chopier J, David J, Lalonde L, Darai E, et al. Nonmasslike enhancement at breast MR imaging: the added value of mammography and US for lesion categorization. *Radiology* 2011;261:69-79
6. Perlet C, Heywang-Kobrunner SH, Heinig A, Sittek H, Casselman J, Anderson I, et al. Magnetic resonance-guided, vacuum-assisted breast biopsy: results from a European multicenter study of 538 lesions. *Cancer* 2006;106:982-990
7. Floery D, Helbich TH. MRI-Guided percutaneous biopsy of breast lesions: materials, techniques, success rates, and management in patients with suspected radiologic-pathologic mismatch. *Magn Reson Imaging Clin N Am* 2006;14:411-425, viii
8. Kuhl C. The current status of breast MR imaging. Part I. Choice of technique, image interpretation, diagnostic accuracy, and transfer to clinical practice. *Radiology* 2007;244:356-378
9. Leung JW. Utility of second-look ultrasound in the evaluation of MRI-detected breast lesions. *Semin Roentgenol* 2011;46:260-274
10. Berg WA, Blume JD, Cormack JB, Mendelson EB. Operator dependence of physician-performed whole-breast US: lesion detection and characterization. *Radiology* 2006;241:355-365
11. Shin HJ, Kim HH, Cha JH. Current status of automated breast ultrasonography. *Ultrasonography* 2015;34:165-172
12. Meng Z, Chen C, Zhu Y, Zhang S, Wei C, Hu B, et al. Diagnostic performance of the automated breast volume scanner: a systematic review of inter-rater reliability/agreement and meta-analysis of diagnostic accuracy for differentiating benign and malignant breast lesions. *Eur Radiol* 2015;25:3638-3647
13. Sim LS, Hendriks JH, Bult P, Fook-Chong SM. US correlation for MRI-detected breast lesions in women with familial risk of breast cancer. *Clin Radiol* 2005;60:801-806
14. Candelaria R, Fornage BD. Second-look US examination of MR-detected breast lesions. *J Clin Ultrasound* 2011;39:115-121
15. Newburg AR, Chhor CM, Young Lin LL, Heller SL, Gillman J, Toth HK, et al. Magnetic resonance imaging-directed ultrasound imaging of non-mass enhancement in the breast: outcomes and frequency of malignancy. *J Ultrasound Med* 2017;36:493-504
16. Carbognin G, Girardi V, Calciolari C, Brandalise A, Bonetti F, Russo A, et al. Utility of second-look ultrasound in the management of incidental enhancing lesions detected by breast MR imaging. *Radiol Med* 2010;115:1234-1245
17. Demartini WB, Eby PR, Peacock S, Lehman CD. Utility of targeted sonography for breast lesions that were suspicious on MRI. *AJR Am J Roentgenol* 2009;192:1128-1134
18. Meissnitzer M, Dershaw DD, Lee CH, Morris EA. Targeted ultrasound of the breast in women with abnormal MRI findings for whom biopsy has been recommended. *AJR Am J Roentgenol* 2009;193:1025-1029
19. Laguna AD, Arranz SJ, Checa VQ, Roca SA, Jiménez DE, Oliver-Goldaracena J. Sonographic findings of additional malignant lesions in breast carcinoma seen by second look ultrasound. *J Clin Imaging Sci* 2011;1:34
20. Mendelson EB, Böhm-Vélez M, Berg WA, Whitman GJ, Feldman MI, Madjar H, et al. ACR BI-RADS(R) ultrasound. In: American College of Radiology. *ACR BI-RADS(R) atlas, breast imaging reporting and data system*. Reston: American College of Radiology, 2013:128-131
21. Sickles EA, D'Orsi CJ, Bassett LW, Appleton CM, Berg WA, Burnside ES, et al. ACR BI-RADS(R) mammography. In: American College of Radiology, eds. *ACR BI-RADS(R) atlas, breast imaging reporting and data system*. Reston: American College of Radiology, 2013:13-120
22. Sakamoto N, Tozaki M, Higa K, Tsunoda Y, Ogawa T, Abe S, et al. Categorization of non-mass-like breast lesions detected by MRI. *Breast Cancer* 2008;15:241-246
23. Baltzer PA, Benndorf M, Dietzel M, Gajda M, Runnebaum IB, Kaiser WA. False-positive findings at contrast-enhanced breast MRI: a BI-RADS descriptor study. *AJR Am J Roentgenol* 2010;194:1658-1663
24. Hsu HH, Chang TH, Chou YC, Peng YJ, Ko KH, Chang WC, et al. Breast nonmass enhancement detected with MRI: uility and lesion characterization with second-look ultrasonography. *Breast J* 2015;21:579-587
25. Spick C, Baltzer PA. Diagnostic utility of second-look US for breast lesions identified at MR imaging: systematic review and meta-analysis. *Radiology* 2014;273:401-409
26. Girometti R, Zanotel M, Londero V, Bazzocchi M, Zuiani C. Comparison between automated breast volume scanner (ABVS) versus hand-held ultrasound as a second look procedure after magnetic resonance imaging. *Eur Radiol* 2017;27:3767-3775
27. Kim Y, Kang BJ, Kim SH, Lee EJ. Prospective study comparing two second-look ultrasound techniques: handheld ultrasound and an automated breast volume scanner. *J Ultrasound Med* 2016;35:2103-2112
28. Chae EY, Shin HJ, Kim HJ, Yoo H, Baek S, Cha JH, et al. Diagnostic performance of automated breast ultrasound as a replacement for a hand-held second-look ultrasound for breast lesions detected initially on magnetic resonance imaging.

https://doi.org/10.3348/kjr.2019.0881

Ultrasound Med Biol 2013;39:2246-2254
29. Halshtok-Neiman O, Shalmon A, Rundstein A, Servadio Y, Gotleib M, Sklair-Levy M. Use of automated breast volumetric sonography as a second-look tool for findings in breast magnetic resonance imaging. *Isr Med Assoc J* 2015;17:410-413
30. Abe H, Schmidt RA, Shah RN, Shimauchi A, Kulkarni K, Sennett CA, et al. MR-directed ("Second-Look") ultrasound examination for breast lesions detected initially on MRI: MR and sonographic findings. *AJR Am J Roentgenol* 2010;194:370-377
31. LaTrenta LR, Menell JH, Morris EA, Abramson AF, Dershaw DD, Liberman L. Breast lesions detected with MR imaging: utility and histopathologic importance of identification with US. *Radiology* 2003;227:856-861

 https://doi.org/10.3348/kjr.2019.0881